Liquid-gas transition and coexistence in ground-state bosons with spin twist

Qi Gu [1,*] and Xiaoling Cui[2,†]

[1]*Institute for Advanced Study, Tsinghua University, Beijing 100084, China*
[2]*Beijing National Laboratory for Condensed Matter Physics, Institute of Physics, Chinese Academy of Sciences, Beijing 100190, China*

We study the thermodynamic liquid-gas transition and coexistence (LGTC) for ground-state bosons under contact interactions. We find that the LGTC can be facilitated by the mismatch of spin polarization, dubbed "spin twist," between single-particle and interaction channels of bosons with spin degrees of freedom. Such a spin twist uniquely stabilizes the gas phase by creating an effective repulsion for low-density bosons, thereby enabling LGTC in the presence of a quantum droplet at a much larger density. We have demonstrated the scheme for binary bosons subject to Rabi coupling and magnetic detuning, where the liquid-gas transition can be conveniently tuned and their coexistence can be characterized by a discontinuous density profile in a harmonic trap. The spin twist scheme for LGTC can be generalized to a wide class of quantum systems with competing single-particle and interaction orders.

Introduction. Liquid-gas transition and coexistence (LGTC) [1] appears to be a common physical phenomenon in nature. Nowadays the phenomenon has many industrial applications in oil, natural gas, aerospace, chemical engineering, etc., and its research has recently even extended to hot nuclei [2–4] and active matters [5,6]. All these systems have two common features. Namely, the LGTCs therein all occur at finite temperature (T) within a certain T window, and they are all associated with long-range interactions characterized by a repulsive core and an attractive tail (e.g., the Lennard-Jones potential), as responsible for the liquid stabilization. Indeed, a textbook model for LGTC is based on the van der Waals' equation of state [7,8], exactly reflecting the important roles played by the thermal effect and long-range potential.

The question is whether we can go beyond the traditional frame to engineer LGTC, so as to broaden the understanding of its nature and enable its potential use in different systems. As a first attempt, Miller *et al.* showed that the liquid-gas transition can occur at zero T where the quantum statistics played a vital role [9,10]. Nevertheless, they still relied on the long-range interaction and concluded the absence of liquid-gas coexistence in bosons given the associated transition is of second order. On the other hand, the recent realization of quantum droplets in ultracold gases [11–21] offers an unprecedented opportunity for addressing the question. These ultracold droplets (with a resemblance to liquids) are stabilized by an attractive mean-field interaction and a repulsive force from quantum fluctuations [22], where the interaction is not necessarily long range but can be a contact one. However, the phenomenon of LGTC has not been deterministically observed in these systems up to date. It is essentially because

the liquid-gas transition therein is continuous at zero T [23], which cannot host any coexistence region as in accordance with Refs. [9,10]. Note that the transitions measured in existing experiments [17–21] are driven by the quantum pressure of a finite-size system, instead of a thermodynamic one. Moreover, since the quantum droplet is quite fragile to the thermal effect [24–26], the LGTC at finite T, even if it exists, can be quite difficult to detect given the expected narrow T window in reality.

In this Letter, we unveil a mechanism for the LGTC of ground-state bosons (zero T) with a contact interaction, thereby well beyond the traditional frame as well as previous theories [9,10]. Such a mechanism is based on a "spin twist," which refers to a mismatch of spin polarization between single-particle and interaction channels for bosons with spin degrees of freedom. To demonstrate the idea, we consider a concrete setup of binary (pseudospin-1/2) ultracold bosons subject to Rabi coupling (Ω) and magnetic detuning (δ) [see the schematics in Fig. 1(a)], as explored in previous experiments [27–31]. The single-particle potentials (Ω, δ) determine an optimal spin polarization, which can be tuned to mismatch the one determined by spin-dependent interactions [Fig. 1(b)]. Such a spin twist leads to an effective repulsion for low-density bosons [Fig. 1(c)], which uniquely stabilizes the gas phase and renders the first-order LGTC in the presence of a quantum droplet at a much larger density [Fig. 1(d)]. In this case, the resulting liquid-gas transitions can be conveniently tuned by Ω, δ and interaction strengths, and moreover, they all occur for thermodynamic systems, in contrast to the finite-size transitions observed previously [17–21]. To characterize the liquid-gas coexistence, we have pointed out their phase separation in a harmonic trap and further identified two universal exponents for the critical scaling of their densities. Our results can be readily detected in ultracold experiments, and the spin twist scheme can serve as a general tool to engineer LGTC in quantum systems.

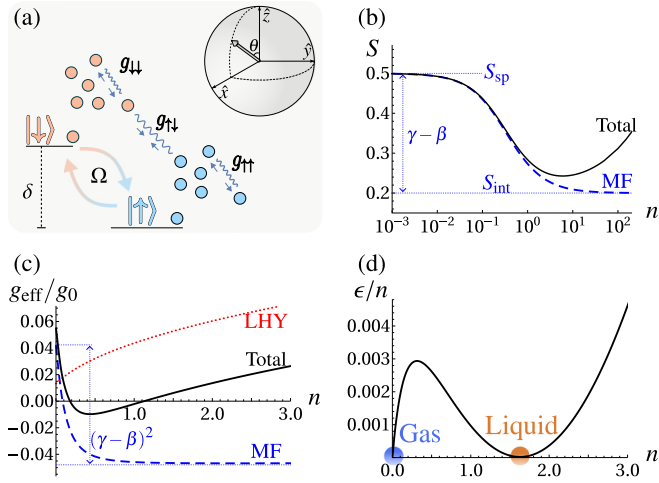*qigu@tsinghua.edu.cn
†xlcui@iphy.ac.cn

FIG. 1. (a) Schematics of a spin twist setup. The spin state of binary bosons, $(\psi_\uparrow, \psi_\downarrow) \propto [\cos(\theta/2), \sin(\theta/2)]$, can be mapped onto a Bloch sphere with polarization $S \equiv \langle \sigma_z \rangle = \cos\theta$. Single-particle potentials $\{\Omega, \delta\}$ and spin-dependent interactions $\{g_{\sigma\sigma'}\}$ respectively optimize θ as θ_{sp} and θ_{int}. A spin twist occurs when $\theta_{sp} \neq \theta_{int}$ and thus $S_{sp} \neq S_{int}$. (b) Density-tuned polarization from $S_{sp}(=\gamma)$ to $S_{int}(=\beta)$. Dashed and solid lines respectively show mean-field and total (with LHY correction) results. (c) Effective interaction (black solid line) and its individual contribution from mean-field (blue dashed) and LHY (red dotted) sectors. The spin twist leads to an additional mean-field repulsion in the low-density regime [$\sim(\gamma - \beta)^2$], as marked by the blue vertical line, which uniquely stabilizes the gas state. (d) Energy per particle (shifted by the single-particle energy $-\sqrt{\Omega^2 + \delta^2}$) as a function of density, where the double minima indicate liquid-gas coexistence near their first-order transition. In (b)–(d) we take the parameters $(\alpha, \beta, \gamma, \eta) = (-0.1, 0.2, 0.5, 0.0137)$, and scale the density and energy per particle respectively by Ω/g_0 and Ω.

Model. We consider the binary bosons ($\uparrow, \downarrow$) with Hamiltonian $H = H_0 + U$ ($\hbar = 1$),

$$H_0 = \int d\mathbf{r} \sum_{\sigma\sigma'} \psi_\sigma^\dagger(\mathbf{r}) \left(-\frac{\nabla^2}{2m} \delta_{\sigma\sigma'} - [\Omega\sigma_x + \delta\sigma_z]_{\sigma\sigma'} \right) \psi_{\sigma'}(\mathbf{r}),$$

$$U = \frac{1}{2} \int d\mathbf{r} \sum_{\sigma\sigma'} g_{\sigma\sigma'} \psi_\sigma^\dagger(\mathbf{r}) \psi_{\sigma'}^\dagger(\mathbf{r}) \psi_{\sigma'}(\mathbf{r}) \psi_\sigma(\mathbf{r}). \quad (1)$$

Here, $\psi_\sigma^\dagger(\mathbf{r})$ is the creation operator of spin-σ, and σ_i ($i = x, y, z$) are Pauli matrices; Ω and δ are respectively the strengths of Rabi coupling and magnetic detuning; $g_{\sigma\sigma'}$ is the contact coupling strength between σ and σ', and here we consider $g_{\uparrow\uparrow}, g_{\downarrow\downarrow} > 0$ and $\delta g \equiv g_{\uparrow\downarrow} + \sqrt{g_{\uparrow\uparrow}g_{\downarrow\downarrow}} < 0$, where a stable quantum droplet can be supported in the absence of Ω and δ [22]. The multiple parameters in this problem can be recombined into four dimensionless ones,

$$\alpha \equiv \frac{\delta g}{g_0}, \quad \beta \equiv \frac{g_{\downarrow\downarrow} - g_{\uparrow\uparrow}}{4g_0},$$

$$\gamma \equiv \frac{\delta}{\sqrt{\delta^2 + \Omega^2}}, \quad \eta \equiv m^3\Omega g_0^2,$$

with $g_0 \equiv (g_{\uparrow\uparrow} + g_{\downarrow\downarrow} - 2g_{\uparrow\downarrow})/4$. Here, α characterizes the strength of an overall attractive interaction; β and γ, as shown later, stand for the optimal spin polarizations in the

interaction and single-particle channels, respectively; η measures the Rabi field with respect to the interaction strength. To simplify the discussions, in this Letter we mainly consider the effects of tunable α and γ.

Spin twist and the induced effective repulsion. Under the mean-field treatment, we replace the field operators by classical numbers, $\psi_\uparrow = \sqrt{n}\cos(\theta/2)$, $\psi_\downarrow = \sqrt{n}\sin(\theta/2)$, where n is the total density, and θ determines the spin polarization,

$$S \equiv \frac{n_\uparrow - n_\downarrow}{n_\uparrow + n_\downarrow} = \cos\theta. \quad (2)$$

The mean-field energy per volume, $\epsilon_{mf} = E_{mf}/V$, is

$$\epsilon_{mf} = -(\sqrt{1 - S^2}\Omega + S\delta)n$$
$$+ \frac{g_0 n^2}{2}\left[(S - \beta)^2 + \frac{g_{\uparrow\uparrow}g_{\downarrow\downarrow} - g_{\uparrow\downarrow}^2}{4g_0^2} \right]. \quad (3)$$

Clearly, the first term contributed from the single-particle potentials favors spin polarization $S_{sp} = \gamma$, while the second term from the interactions favors $S_{int} = \beta$. A "spin twist" occurs when the two polarizations are mismatched, i.e., $\beta \neq \gamma$. The overall mean-field polarization, as determined by $\partial\epsilon_{mf}/\partial S = 0$, is shown by the dashed line in Fig. 1(b), which is density dependent and can change from γ to β as n increases.

A remarkable effect of such a spin twist is to induce an effective repulsion uniquely in the low-density limit. Here, we define the effective interaction as

$$g_{eff} \equiv \frac{\partial^2\epsilon}{\partial n^2}, \quad (4)$$

where ϵ is the energy density after optimizing S. In the absence of spin twist, the two terms in Eq. (3) both favor $S = \beta = \gamma$, leading to $g_{eff,mf}^{(0)} = (g_{\uparrow\uparrow}g_{\downarrow\downarrow} - g_{\uparrow\downarrow}^2)/(4g_0)$. This is the conventional case of binary bosons, whose mean-field stability is given by $g_{\uparrow\uparrow}g_{\downarrow\downarrow} > g_{\uparrow\downarrow}^2$ for any density. However, it is no longer true when a spin twist occurs ($\beta \neq \gamma$). In this case, the single-particle and interaction terms compete with each other and the resulting S and $g_{eff,mf}$ are generally n dependent. In the low-n limit, the single-particle terms dominate, which results in $S \sim \gamma$ and

$$g_{eff,mf} = g_{eff,mf}^{(0)} + g_0(\gamma - \beta)^2. \quad (5)$$

Here, the spin twist leads to an additional repulsion $\sim g_0(\gamma - \beta)^2$ at the mean-field level. Its physical origin can be understood as follows: Since the interactions favor $S \sim \beta$ as the ground state, here $S \sim \gamma$ corresponds to an excited spin orientation in the interaction channel, which naturally generates an effective repulsion as above. Note that such repulsion only works for low densities but not high ones, where the interactions dominate and recover $S \sim \beta$ and $g_{eff,mf} \sim g_{eff,mf}^{(0)}$.

Beyond the mean-field treatment, we have further carried out the Bogoliubov analysis and extracted the Lee-Huang-Yang (LHY) energy ϵ_{LHY} from quantum fluctuations [32]. In Fig. 1(c), we plot out the typical n-dependent g_{eff} obtained from the total $\epsilon = \epsilon_{mf} + \epsilon_{LHY}$, as well as its individual contributions from the mean-field and LHY parts. As expected, the mean-field contribution $g_{eff,mf}$ is positive only in the low-n limit, and gradually reduces to a negative value as n increases. The reduction is exactly given by $\sim g_0(\gamma - \beta)^2$ due to the spin
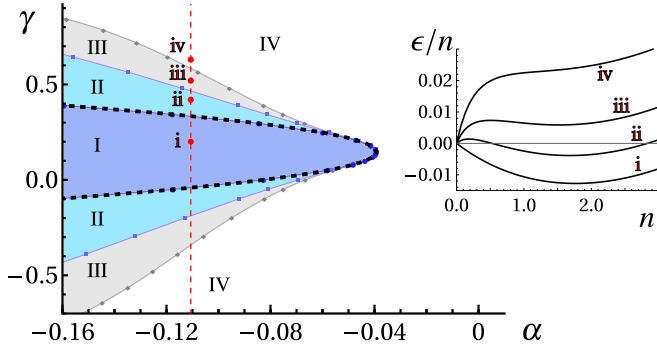
FIG. 2. Ground-state phase diagram in the (α, γ) plane with fixed $\beta = 0.141$, $\eta = 0.0157$. Here, I–IV respectively denote the region where the ground state is a pure droplet, a droplet with a metastable gas, a gas with a metastable droplet, and a pure gas. The liquid-gas transition occurs at the II-III boundary. The inset shows typical $\epsilon/n(n)$ curves for different regions, as marked by i–iv in the main plot. For each curve ϵ/n is shifted by a single-particle energy $(-\sqrt{\Omega^2 + \delta^2})$. We scale n and ϵ/n respectively by Ω/g_0 and Ω.

twist [Eq. (5)]. In comparison, the LHY contribution $g_{\text{eff,LHY}}$ is always positive and continuously grows with n. The total g_{eff} then displays an intriguing sign change as n increases: It turns from positive to negative, and back to positive again at large n. Consequently, the energy per particle ϵ/n as a function of n displays double minima [see Fig. 1(d)]. Here, the second minimum at finite n is a self-bound droplet with zero pressure that is mainly balanced by a mean-field attraction and LHY repulsion, sharing the same spirit as an ordinary case [22], while the first minimum at $n = 0$ stands for a gas stabilized by a unique low-n repulsion under a spin twist [cf. Eq. (5)]. Such a double-minima structure implies a first-order transition between liquid and gas as well as their coexistence under proper conditions. We have checked that a similar structure cannot appear without a spin twist [32].

From the dressed basis perspective, the gas with $n \sim 0$ and $S \sim \gamma$ essentially occupies the lowest dressed branch as explored in experiments [28–30], while for the liquid phase at finite n, whose polarization can be far from γ, the single dressed branch is generally not a good description due to the considerable population at the higher branch.

Ground-state phase diagram. The ground state (gas or self-bound droplet) is given by the global minimum in the $\epsilon/n(n)$ curve, which is associated with the lowest chemical potential $\mu = \partial\epsilon/\partial n = \epsilon/n$. In Fig. 2, we present the ground-state phase diagram in the (α, γ) plane for a given set of β, η. Four phases are shown, i.e., a pure droplet (I), a droplet with a metastable gas (II), a gas with a metastable droplet (III), and a pure gas (IV). Typical $\epsilon/n(n)$ landscapes for different regions are given in the inset plot. The double-minima structure appears in regions II and III, and the liquid-gas transition occurs at the II-III boundary when they have the same $\epsilon/n = \mu = -\sqrt{\Omega^2 + \delta^2}$, i.e., the single-particle shift.

We would like to remark on a crucial difference between the liquid-gas transition here and those observed previously in binary bosons [17–21]. In previous cases, the transition is driven by the gradually dominant quantum pressure as compared to interaction terms when the boson number N decays, and therefore it occurs for finite-size systems when N reaches
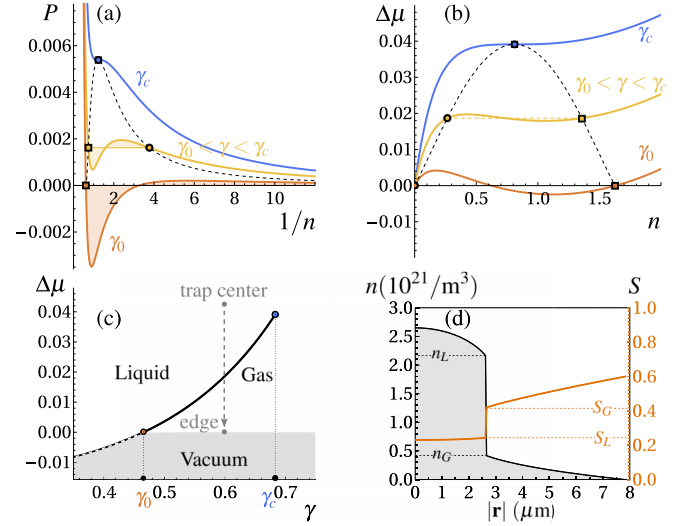

FIG. 3. Liquid-gas coexistence(LGC) tuned by γ at fixed $\alpha = -0.11$, $\beta = 0.141$, $\eta = 0.0157$. (a) Pressure P as a function of $1/n$ for different $\gamma = 0.465(= \gamma_0)$, 0.6, 0.683($= \gamma_c$) (from bottom to top). (b) Shifted chemical potential $\Delta\mu \equiv \mu + \sqrt{\Omega^2 + \delta^2}$ as a function of n for different γ as in (a). The intersections between these curves and horizontal lines in (a) and (b) give the equilibrium densities of liquid (n_L, squares) and gas (n_G, circles), which are connected by binodal lines (dashed). For each curve in (a), the two shadow regions have the same area following the Maxwell's construction. (c) Phase diagram of liquid, gas, and vacuum in the $(\gamma, \Delta\mu)$ plane. LGC occurs along the black line for $\gamma \in (\gamma_0, \gamma_c)$. At $\gamma < \gamma_0$, only a self-bound droplet (liquid) is present if $\Delta\mu$ is above the dashed line. At $\gamma > \gamma_c$, the liquid and gas are indistinguishable. (d) Profiles of total density (n) and spin polarization (S) for bosons in an isotropic harmonic trap with frequency $\omega = (2\pi)50$ Hz, total number $N = 4 \times 10^5$, and $\gamma = 0.6$, corresponding to the vertical trajectory shown in (c). The sharp jumps of n and S mark the location of LGC. For all plots, we scale the density and energy per particle respectively by Ω/g_0 and Ω.

a critical value. However, in our case the transition occurs in the thermodynamic limit ($N, V \to \infty$ with $n = N/V$) and is driven by the competition between single-particle and interaction potentials. Therefore, the current case allows a highly tunable transition point for an arbitrarily large system, and moreover, allows for the exploration of liquid-gas coexistence in a considerably broad parameter regime, as shown below.

Liquid-gas coexistence. We now analyze the properties of bosons confined in a harmonic trap. We consider a realistic system of ^{39}K atoms with hyperfine states $|F = 1, m_F = -1\rangle \equiv |\uparrow\rangle$, $|F = 1, m_F = 0\rangle \equiv |\downarrow\rangle$, as well studied in ultracold droplet experiments [17–19]. In this system, $a_{\uparrow\uparrow} = 35a_0$, $a_{\uparrow\downarrow} = -53a_0$ (a_0 is the Bohr radius), and $a_{\downarrow\downarrow}$ is highly tunable by magnetic field. For a concrete demonstration, here we take $a_{\downarrow\downarrow} = 64a_0$, $\Omega = (2\pi)3.5$ kHz (thus α, β, η are all fixed), and only focus on the coexistence region tuned by δ (or γ).

The coexistence of liquid and gas requires

$$\mu(n_L) = \mu(n_G), \quad P(n_L) = P(n_G), \quad (6)$$

where n_L (n_G) is the liquid (gas) density at equilibrium, μ is the chemical potential, and $P = \mu n - \epsilon$ is the pressure. In Figs. 3(a) and 3(b), we plot out $P(1/n)$ and $\mu(n)$ for several

typical γ. We can see that $P(1/n)$ shows a similar line shape as classical P-V isotherms hosting LGTC [7,8]. Here, we have used the Maxwell's construction to identify n_L and n_G, as marked respectively by squares and circles in Fig. 3(a). Specifically, n_L (n_G) is given by the left (right) intersection between each $P(1/n)$ curve and a horizontal line, by requiring the same area of two separated shadow regions. The relation $\int d\mu = \int 1/n dP$ then guarantees the same μ at the intersections [see also Fig. 3(b)], which will be denoted as μ_{LGC} from now on.

Figures 3(a) and 3(b) also indicate a finite parameter window, $\gamma \in (\gamma_0, \gamma_c)$, for the occurrence of liquid-gas coexistence. At the lower bound γ_0, a gas phase starts to emerge at $n_G = 0$ and the two phases have $\mu = -\sqrt{\Omega^2 + \delta^2}$ and $P = 0$. This is right at the ground-state transition between the liquid and gas, i.e., at the II-III boundary shown in Fig. 2. As increasing γ, the coexisting phases have higher μ, P and meanwhile n_G and n_L get closer. Finally, the coexistence terminates at the critical point γ_c when n_L, n_G merge into a single value (n_c) at the inflections of $\mu(n)$ and $P(1/n)$ curves. For even larger $\gamma > \gamma_c$, the gas and liquid become indistinguishable.

Figure 3(c) further summarizes the results in the (γ, μ) plane, where μ_{LGC} (solid line) separates the liquid and gas for $\gamma \in (\gamma_0, \gamma_c)$. To observe their coexistence, we suggest measuring the density profiles of bosons under an external trap, and here for brevity we consider an isotropic harmonic trap $V(\mathbf{r}) = m\omega^2 \mathbf{r}^2/2$. Using the local density approximation $\mu(\mathbf{r}) = \mu(0) - V(\mathbf{r})$, in Fig. 3(d) we plot out the typical profiles of n and S in the trap showing the liquid-gas phase separation, where the liquid and gas respectively occupy the trap center and edge. At their interface n (S) displays a sharp jump from n_L to n_G (S_L to S_G), marking the location of liquid-gas coexistence with $\mu = \mu_{LGC}$. Note that $n_{L,G}$ and $S_{L,G}$ do not depend on a specific boson number N, as long as it is above a critical value [32].

Interestingly, the liquid and gas obey a universal critical scaling near the melting of LGTC. Here, we explore the asymptotic behavior of their relative and mean densities near $\gamma \sim \gamma_c$ and $n_L \sim n_G \sim n_c$,

$$\frac{n_L - n_G}{n_c} \propto (\gamma_c - \gamma)^\lambda, \quad \frac{n_L + n_G}{2n_c} - 1 \propto (\gamma_c - \gamma)^\xi, \quad (7)$$

with λ, ξ the corresponding critical exponents. In Figs. 4(a) and 4(b), we have numerically extracted the exponents as $\lambda = 1/2$ and $\xi = 1$ for all given α. These exponents also universally persist for other tunable parameters, such as changing γ to α [32]. To explain such a universal phenomenon, we have adopted a mean-field theory as in the classical treatment of the finite-T liquid-gas transition [1], which well predicts the universal critical exponents as above [32].

Here, we clarify that the liquid-gas coexistence here should be distinguished from the equilibrium of a droplet and a fully polarized gas in previous studies [33–36], where Ω, δ are
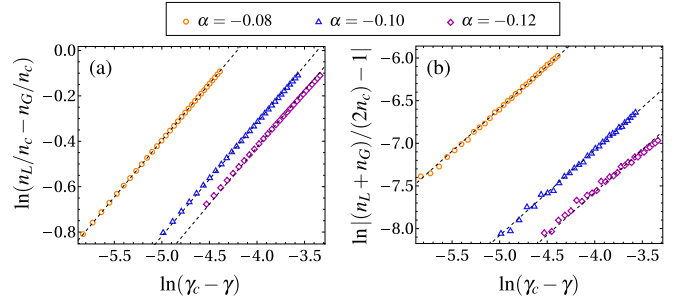

FIG. 4. Universal critical scaling for the (a) relative and (b) averaged densities of liquid and gas at their coexistence. β, η are the same as in Fig. 3. Discrete points show numerical data and dashed lines show linear fittings. Here, we take a ln - ln plot, and the slopes for all fitting lines in (a) are $1/2$ and in (b) are 1, giving the corresponding exponents λ and ξ defined in Eq. (7).

both absent. The latter is due to a preset spin population that deviates from the one preferred by the droplet, and therefore the residue (single-species) bosons are repelled out of the droplet to form a gas. In contrast, the coexistence here is associated with a first-order liquid-gas transition (Fig. 1), where the spin population is changeable and both species can transfer freely between two phases to reach mutual equilibration.

Summary. We have revealed a mechanism using spin twist to engineer liquid-gas transition and coexistence (LGTC) in ground-state bosons, which does not rely on a thermal effect or long-range potential. The scheme is demonstrated with a specific model of binary bosons under Rabi coupling and magnetic detuning. Taking the realistic ^{39}K atoms for example, in practice one can follow the strategy in Refs. [28–30] to prepare a gas at the ground state, from which a liquid (droplet) can be approached by changing γ or α following Fig. 2. The LGTC naturally occurs during this process, and the proposed phase separation in a trap and the universal scaling of equilibrium densities can be readily tested in experiments.

Finally, we remark that the spin twist in creating an effective low-density repulsion for gas stabilization is a very robust mechanism, which can be applied to a wide class of quantum systems with competing single-particle and interaction orders. For instance, it is expected to still work when adding more spin degrees of freedom, or changing Ω, δ to other single-particle potentials in altering spins. In this regard, the spin twist can serve as a general principle for achieving LGTC at ultralow temperatures, which hopefully would promote the practical use of such phenomena in a fascinating quantum world in the future.

---

[1] P. M. Chaikin and T. C. Lubensky, *Principles of Condensed Matter Physics* (Cambridge University Press, Cambridge, UK, 1995).

[2] J. Richert and P. Wagner, Microscopic model approaches to fragmentation of nuclei and phase transitions in nuclear matter, Phys. Rep. **350**, 1 (2001).

[3] V. A. Karnaukhov, H. Oeschler, S. P. Avdeyev, E. V. Duginova, V. K. Rodionov, A. Budzanowski, W. Karcz, O. V. Bochkarev, E. A. Kuzmin, L. V. Chulkov, E. Norbeck, and A. S. Botvina, Critical temperature for the nuclear liquid-gas phase transition, Phys. Rev. C **67**, 011601(R) (2003).

[4] V. Vovchenko, M. I. Gorenstein, and H. Stoecker, van der Waals Interactions in Hadron Resonance Gas: From Nuclear Matter to Lattice QCD, Phys. Rev. Lett. **118**, 182301 (2017).

[5] M. E. Cates and J. Tailleur, Motility-induced phase separation, Annu. Rev. Condens. Matter Phys. **6**, 219 (2015).

[6] A. K. Omar, K. Klymko, T. GrandPre, and P. L. Geissler, Phase Diagram of Active Brownian Spheres: Crystallization and the Metastability of Motility-Induced Phase Separation, Phys. Rev. Lett. **126**, 188002 (2021).

[7] L. D. Landau and E. M. Lifshitz, *Statistical Physics (Part 1)*, 3rd ed. (Elsevier, Singapore, 2007).

[8] K. Huang, *Statistical Mechanics*, 2nd ed. (Wiley, New York, 1991).

[9] M. D. Miller, L. H. Nosanow, and L. J. Parish, Liquid-to-Gas Phase Transition in Quantum Systems at Zero Temperature, Phys. Rev. Lett. **35**, 581 (1975).

[10] M. D. Miller and L. H. Nosanow, Liquid-to-gas phase transitions in two-dimensional quantum systems at zero temperature, J. Low Temp. Phys. **32**, 145 (1978).

[11] I. Ferrier-Barbut, H. Kadau, M. Schmitt, M. Wenzel, and T. Pfau, Observation of Quantum Droplets in a Strongly Dipolar Bose Gas, Phys. Rev. Lett. **116**, 215301 (2016).

[12] M. Schmitt, M. Wenzel, F. Böttcher, I. Ferrier-Barbut, and T. Pfau, Self-bound droplets of a dilute magnetic quantum liquid, Nature (London) **539**, 259 (2016).

[13] L. Chomaz, S. Baier, D. Petter, M. J. Mark, F. Wächtler, L. Santos, and F. Ferlaino, Quantum-Fluctuation-Driven Crossover from a Dilute Bose-Einstein Condensate to a Macro-droplet in a Dipolar Quantum Fluid, Phys. Rev. X **6**, 041039 (2016).

[14] L. Tanzi, E. Lucioni, F. Fama, J. Catani, A. Fioretti, C. Gabbanini, R. N. Bisset, L. Santos, and G. Modugno, Observation of a Dipolar Quantum Gas with Metastable Supersolid Properties, Phys. Rev. Lett. **122**, 130405 (2019).

[15] F. Böttcher, J.-N. Schmidt, M. Wenzel, J. Hertkorn, M. Guo, T. Langen, and T. Pfau, Transient Supersolid Properties in an Array of Dipolar Quantum Droplets, Phys. Rev. X **9**, 011051 (2019).

[16] L. Chomaz, D. Petter, P. Ilzhöfer, G. Natale, A. Trautmann, C. Politi, G. Durastante, R. M. W. van Bijnen, A. Patscheider, M. Sohmen, M. J. Mark, and F. Ferlaino, Long-Lived and Transient Supersolid Behaviors in Dipolar Quantum Gases, Phys. Rev. X **9**, 021012 (2019).

[17] C. R. Cabrera, L. Tanzi, J. Sanz, B. Naylor, P. Thomas, P. Cheiney, and L. Tarruell, Quantum liquid droplets in a mixture of Bose-Einstein condensates, Science **359**, 301 (2018).

[18] P. Cheiney, C. R. Cabrera, J. Sanz, B. Naylor, L. Tanzi, and L. Tarruell, Bright Soliton to Quantum Droplet Transition in a Mixture of Bose-Einstein Condensates, Phys. Rev. Lett. **120**, 135301 (2018).

[19] G. Semeghini, G. Ferioli, L. Masi, C. Mazzinghi, L. Wolswijk, F. Minardi, M. Modugno, G. Modugno, M. Inguscio, and M. Fattori, Self-Bound Quantum Droplets of Atomic Mixtures in Free Space, Phys. Rev. Lett. **120**, 235301 (2018).

[20] C. D'Errico, A. Burchianti, M. Prevedelli, L. Salasnich, F. Ancilotto, M. Modugno, F. Minardi, and C. Fort, Observation of quantum droplets in a heteronuclear bosonic mixture, Phys. Rev. Res. **1**, 033155 (2019).

[21] Z. Guo, F. Jia, L. Li, Y. Ma, J. M. Hutson, X. Cui, and D. Wang, Lee-Huang-Yang effects in the ultracold mixture of ^{23}Na and ^{87}Rb with attractive interspecies interactions, Phys. Rev. Res. **3**, 033247 (2021).

[22] D. S. Petrov, Quantum Mechanical Stabilization of a Collapsing Bose-Bose Mixture, Phys. Rev. Lett. **115**, 155302 (2015).

[23] For thermodynamic boson mixtures, the equilibrium density of a quantum droplet continuously goes to zero (gas) as the system is tuned across the mean-field collapse point [22]. This marks a continuous, rather than a first-order, liquid-gas transition at this point.

[24] M. Ota and G. Astrakharchik, Beyond Lee-Huang-Yang description of self-bound Bose mixtures, SciPost Phys. **9**, 020 (2020).

[25] J. Wang, X.-J. Liu, and H. Hu, Ultradilute self-bound quantum droplets in Bose-Bose mixtures at finite temperature, Chin. Phys. B **30**, 010306 (2021).

[26] N. Guebli and A. Boudjemâa, Quantum self-bound droplets in Bose-Bose mixtures: Effects of higher-order quantum and thermal fluctuations, Phys. Rev. A **104**, 023310 (2021).

[27] E. Nicklas, H. Strobel, T. Zibold, C. Gross, B. A. Malomed, P. G. Kevrekidis, and M. K. Oberthaler, Rabi Flopping Induces Spatial Demixing Dynamics, Phys. Rev. Lett. **107**, 193001 (2011).

[28] L. Lavoine, A. Hammond, A. Recati, D. S. Petrov, and T. Bourdel, Beyond-Mean-Field Effects in Rabi-Coupled Two-Component Bose-Einstein Condensate, Phys. Rev. Lett. **127**, 203402 (2021).

[29] A. Hammond, L. Lavoine, and T. Bourdel, Tunable Three-Body Interactions in Driven Two-Component Bose-Einstein Condensates, Phys. Rev. Lett. **128**, 083401 (2022).

[30] J. Sanz, A. Frölian, C. S. Chisholm, C. R. Cabrera, and L. Tarruell, Interaction Control and Bright Solitons in Coherently Coupled Bose-Einstein Condensates, Phys. Rev. Lett. **128**, 013201 (2022).

[31] R. Cominotti, A. Berti, C. Dulin, C. Rogora, G. Lamporesi, L. Carusotto, A. Recati, A. Zenesini, and G. Ferrari, Revealing the ferromagnetic phase transition in an extended two-component atomic superfluid, arXiv:2209.13235.

[32] See Supplemental Material at http://link.aps.org/supplemental/10.1103/PhysRevA.107.L031303 for more detailed discussions on beyond-mean-field correction, liquid-gas coexistence in trapped system and universal scaling near the critical point.

[33] T. Mithun, A. Maluckov, K. Kasamatsu, B. A. Malomed, and A. Khare, Modulational instability, intercomponent asymmetry, and formation of quantum droplets in one-dimensional binary Bose gases, Symmetry **12**, 174 (2020).

[34] M. N. Tengstrand and S. M. Reimann, Droplet-superfluid compounds in binary bosonic mixtures, Phys. Rev. A **105**, 033319 (2022).

[35] T. A. Flynn, L. Parisi, T. P. Billam, and N. G. Parker, Quantum droplets in imbalanced atomic mixtures, arXiv:2209.04318.

[36] L. He, H. Li, W. Yi, and Z.-Q. Yu, Quantum criticality of liquid-gas transition in a binary boson mixture, arXiv:2209.13559.